

Minimizing Elastic Energy of a Model Cytoskeleton Network

With Fast Inertial Relaxation Engine(FIRE) Algorithm

Hins Qiu

A senior thesis submitted to the faculty of the
University of California, Merced
in partial fulfillment of the requirements for the degree of

Bachelor of Science

Kinjal Dasbiswas, PhD

Department of Physics

University of California, Merced

December 2024

Copyright © 2024 Hins Qiu

All Rights Reserved

ABSTRACT

Minimizing Elastic Energy of a Model Cytoskeleton Network With Fast Inertial Relaxation Engine(FIRE) Algorithm

Hins Qiu

Department of Physics, UCM
Bachelor of Science

Myosin II is a motor protein that generates mechanical forces to facilitate various cellular processes in animal cells. These processes include cell adhesion, migration, and muscle contraction. Myosin II mainly interacts with actin filaments in the cytoskeleton— a disordered, viscoelastic network of protein filaments found in many animal cells. The actin-myosin interactions produce forces that propagate throughout the cytoskeleton. These forces are potentially responsible for the ordered self-organization of the cytoskeleton. To understand such organizations, we examine a percolated fiber lattice model, where fibers are simplified as linear elastic elements that can both stretch and compress. The contractile activity of myosin II is represented by force dipoles. By varying the amounts of fibers and dipoles, we analyze how their mechanical deformations change the overall structure of the lattice. Using the Fast Inertial Relaxation Engine(FIRE) algorithm, We observed the characteristic patterns of force propagation with stretched bonds distributed radially and compressed bonds, distributed transversely. The model can be used to study how cell contractility depends on cytoskeletal architecture.

Contents

Table of Contents	iii
1 Introduction	1
1.1 Motivation	1
1.2 Background	3
2 Method	6
2.1 Model	6
2.2 Molecular Dynamics(MD)	7
2.3 Fast Inertial Relaxation Engine(FIRE)	8
3 Results	9
3.1 4x4 Network	9
3.2 32x32 Network	10
3.3 64x64 Newwork and multiple dipoles	13
4 Conclusion	16
4.1 Summary	16
4.2 Future Work	17
Bibliography	18

Chapter 1

Introduction

1.1 Motivation

This project aims to explore the FIRE computational model in achieving energy optimization in a triangular lattice of elastic springs subject to local deformations. Such a lattice model has been used to model fibrous biopolymer networks such as the cell cytoskeleton and extracellular matrix [1], which are subject to myosin motor-induced mechanical deformation. FIRE has demonstrated greater efficiency in reaching energy minimum than other traditional methods such as conjugated gradients (CG) and the limited memory Broyden-Fletcher-Goldfarb-Shanno (L-BFGS) scheme. [2] We also compared FIRE with another technique called steepest descent(SD), and we found similar results in which FIRE finished the minimization much faster than SD in a one-spring system.(Figure 1.2)

1.1 Motivation

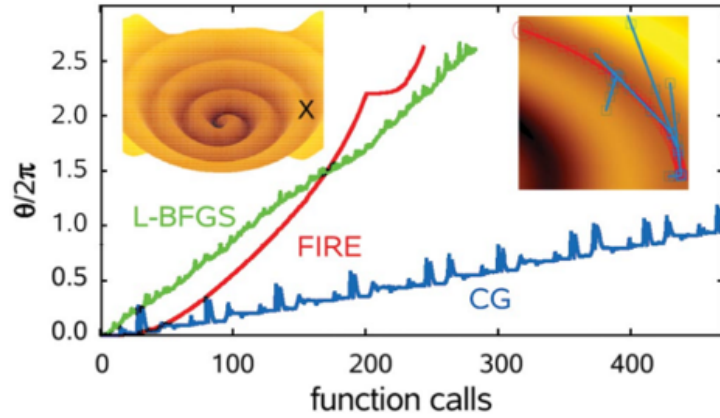


Figure 1.1 The optimization of a spiral-shaped potential energy function begins at point X. The graph illustrates how the azimuthal angle θ changes with the number of function calls for three methods: FIRE, CG, and L-BFGS. Initially, FIRE progresses more slowly, but it rapidly gains speed and matches L-BFGS as the curvature increases. Conversely, CG fails to converge within 500 function calls due to inefficient line searches, as shown in the right inset which highlights part of the trajectories of FIRE and CG. [2]

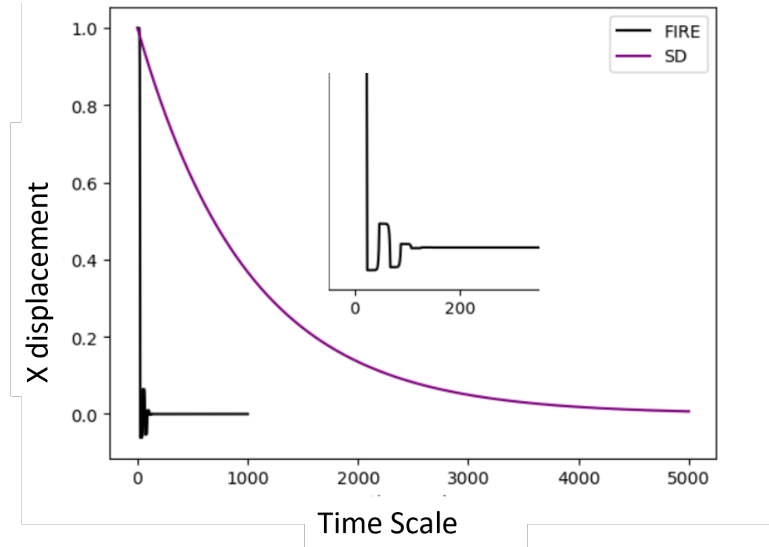


Figure 1.2 The optimization of a single-spring potential energy function. The graph illustrates how the spring has some initial oscillation and stabilizes around 200 time steps in FIRE, the middle is the zoom-in version to visualize the oscillation better. SD on the other hand shows a gradual decrease and is more than 20 times slower in reaching minimum than FIRE.

1.2 Background

1.2 Background

The cytoskeleton is a complex and dynamic network constituted by various protein filaments in all cells' cytoplasm. These protein filaments have 3 main categories: actin filaments, intermediate filaments, and microtubules, and can rapidly assemble and disassemble to produce essential functions such as cell motility, shape change, and cell division. In particular, myosin II is important in generating force interactions among these filaments. [3] Myosin II consumes an energy source called adenosine triphosphate(ATP) and crawls on the actin, creating a force dipole with the polarity of the actin, allowing the cell to stretch and compress to generate cellular functions.

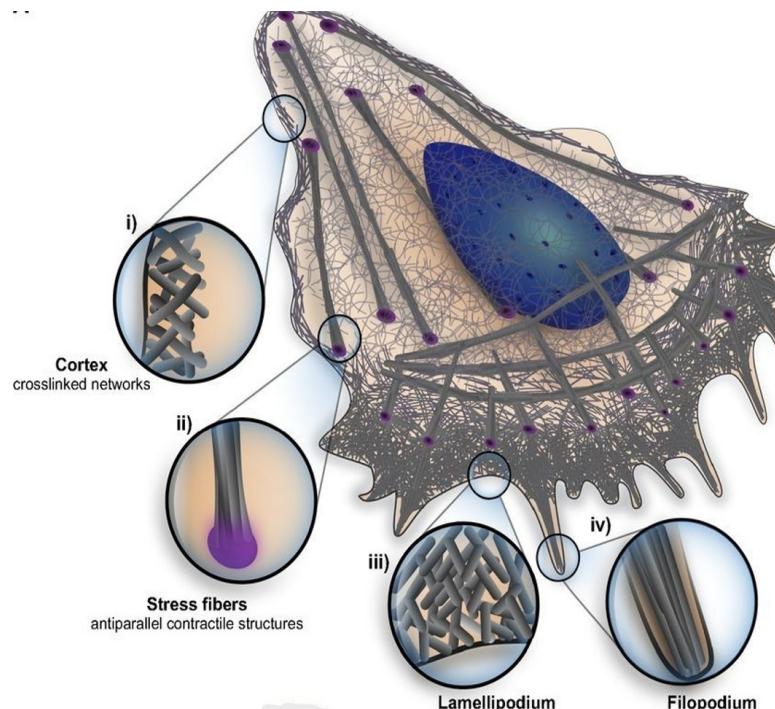


Figure 1.3 Experimental results showing ordered structure of actomyosin network in non-muscle cells. It was found in the experiment that molecular motor forces were crucial in this stacking. The cell and its cytoskeleton structures as depicted: i) the cell cortex; ii) a contractile fiber known as the stress fiber; iii) the lamellipodium; and iv) the filopodium. [3]

1.2 Background

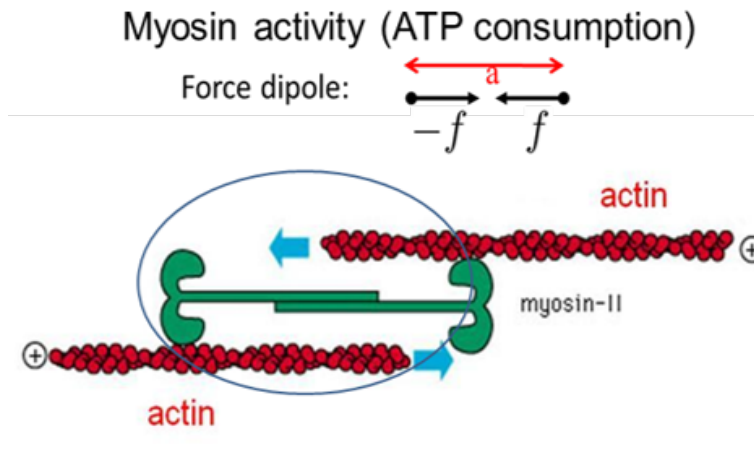


Figure 1.4 Myosin motors(green) exert forces by sliding acting according to polarity of the actins(red). These forces generated by myosins are crucial for the ordering seen in Figure 1.3 [3]

A simplified model for cellular force distribution across different spatial scales, whether from individual actomyosin units in the cytoskeleton or entire cells attached to an extracellular matrix, involves a contractile force dipole within an elastic medium as shown in Figure 1.4. The spatial distribution of deformation caused by this force dipole, such as the extent of strain propagation from the dipole, depends on the mechanical properties of the medium. In fibrous networks like the extracellular matrix made of collagen or fibrin, force transmission can extend further than in a linear elastic medium. The enhanced range of force transmission is believed to result from the compression-induced softening of fibers due to buckling, along with their stiffening under tension. Understanding how forces propagate from an active contractile force dipole through a heterogeneous elastic medium and how this facilitates mechanical interaction between distant force dipoles are key biophysical questions. This is comparable to the elastic interaction of defects that generate stress in passive materials and contribute to the organization of other disordered media like granular packings.

On short time scales, before cytoskeletal remodeling occurs, the cytoskeleton acts as an elastic material capable of sustaining and transmitting mechanical stresses. The disordered cytoskeleton

1.2 Background

can be modeled as a network of elastic fibers resisting stretching, characterized by elastic modulus μ . When fibers are much shorter than their persistence length, thermal fluctuations can be neglected, allowing an athermal, linear elastic model to describe the cytoskeletal network instead of the nonlinear, entropic elastic behavior of semiflexible polymers. This model can be extended to include nonlinear constitutive relations for a more realistic representation of cytoskeletal filaments. However, for small deformations far from the dipole, the force-extension relationship of each fiber is likely to remain linear. [4]

Chapter 2

Method

2.1 Model

To run the simulations, we used Python version 3.11.10 and Spyder version 6.0.3. We simulate an elastic network with a triangular lattice where each bond represents a spring. We started with one dipole at the center with free boundaries condition, and later we added fixed boundary condition as well. We calculate the elastic energy of the network as followed:

$$E = \frac{\mu}{2} \sum_{\langle ij \rangle} (r_{ij} - r_0)^2 \quad (2.1)$$

where μ is the stretching modulus of the spring, r_{ij} represents the length of the bond connecting two neighboring nodes, and r_0 is its rest length, ordinarily set to 1. To create deformation in the network, we introduce “isotropic force dipoles” by reducing the rest length of all six bonds around the “active node” to $l_0 = 0.9$. If the bond is stretched, we label it blue, if it’s compressed, we label it red, and the nodes of the dipoles are labeled green as shown in Figure 2.1. [4]

2.2 Molecular Dynamics(MD)

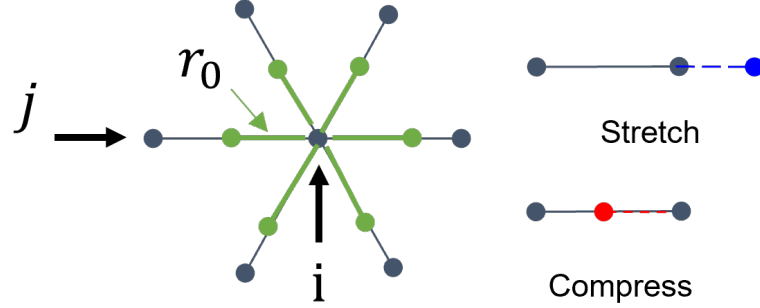


Figure 2.1 "Illustration of the connectivity within the lattice, where the inner node is labeled i , while the outer nodes are labeled j . The dipole is labeled green, and its rest length r_0 is shorter than the rest of the network, so its bonds r_{ij} are always stretched. We label the bond blue if it has been stretched, and red if it has been compressed."

2.2 Molecular Dynamics(MD)

Each node in the spring network is moved in FIRE simulations in a molecular dynamics step. In molecular dynamics, we use Velocity Verlet, a common numerical method in physics to calculate Newton's equations of motion. We update the position \vec{x} and velocity \vec{v} based on their previous values and the acceleration \vec{a} . The equations of motion in arbitrary dimensions in discretized form are as follows:

$$\vec{x}(t + \Delta t) = \vec{x}(t) + \vec{v}(t)\Delta t + \frac{\vec{a}(t)\Delta t^2}{2}, \quad (2.2)$$

,

$$\vec{v}(t + \Delta t) = \vec{v}(t) + (\vec{F}/m)\Delta t \quad (2.3)$$

where m is the mass of a fictitious particle at the node, and \vec{F} is the force acting on the node, which includes both viscous and elastic contributions.

The net force on the i^{th} node can be written as

$$\vec{F}_i = -\gamma \vec{v}_i - \mu \sum_{\langle ij \rangle} (r_{ij} - r_0) \hat{r}_{ij}, \quad (2.4)$$

2.3 Fast Inertial Relaxation Engine(FIRE)

where the viscous force involves the friction coefficient γ modeling the solvent drag on a moving particle, and the elastic forces are derived from the potential energy in Eq. 2.1.

2.3 Fast Inertial Relaxation Engine(FIRE)

F1: calculate $P = \mathbf{F} \cdot \mathbf{v}$.
F2: set $\mathbf{v} \rightarrow (1 - \alpha)\mathbf{v} + \alpha\hat{\mathbf{F}}|\mathbf{v}|$.
F3: if $P > 0$ and the number of steps since P was negative is larger than N_{\min} , increase the time step $\Delta t \rightarrow \min(\Delta t f_{\text{inc}}, \Delta t_{\max})$ and decrease $\alpha \rightarrow \alpha f_{\alpha}$.
F4: if $P \leq 0$, decrease time step $\Delta t \rightarrow \Delta t f_{\text{dec}}$, freeze the system $\mathbf{v} \rightarrow 0$ and set α back to α_{start} .
F5: return to MD.
MD: calculate \mathbf{x} , $\mathbf{F} = -\nabla E(\mathbf{x})$, and \mathbf{v} using any common MD integrator; check for convergence.

Figure 2.2 The basic workflow of FIRE, in which we start with FIRE and then followed by MD. The sequence of FIRE is labeled as F1-F5.

The general idea of FIRE can be thought as going uphill or downhill in an energy landscape (Figure 2.2). To distinguish uphill and downhill, we calculate the power(P) of the system using force(\mathbf{F}) dotted with velocity(\mathbf{v}) in F1. Power greater than zero is considered downhill(F3), and there must be some latency N_{\min} between uphill and downhill to ensure a smoother transition. If we are traveling downhill, we carry some of the inertia from the previous time-step($(1 - \alpha)v$ in F2), and then we accelerate in the same direction as the force($\alpha\hat{\mathbf{F}}|\mathbf{v}|$ in F2). " α " is a built-in constant to modify the amount of inertia. Now we can accelerate the simulation with greater time step Δt and decrease α to carry a bigger inertia. If we are traveling uphill, that is, not in the direction of minimizing energy, we stop($v = 0$) and look for a different direction, and we want to be more careful in finding the right direction by decreasing Δt and set α as how it started. After FIRE, there's MD to update the position and velocity of every node and it will loop through FIRE until the maximum time-step is reached.

Chapter 3

Results

3.1 4x4 Network

To test out FIRE, we started with a small network of dimension "4x4", meaning 4 nodes on the x-axis and 4 nodes on the y-axis and a total of $4 \times 4 = 16$ nodes.

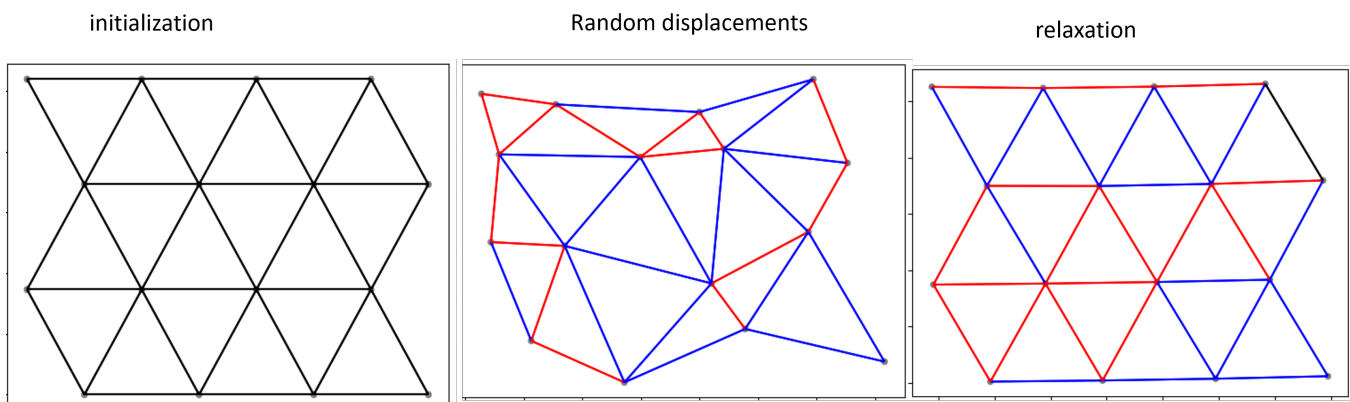


Figure 3.1 "Illustration of a 4x4 network transforming back to its original structure after undergoing random displacements. The leftmost graph displays the initial regular triangular mesh, the middle graph shows the distorted mesh with each of the 16 nodes randomly displaced, and the rightmost graph represents the mesh approaching its original form."

3.2 32x32 Network

After establishing that our FIRE code works for a small network, we next considered a 32x32 network with one isotropic force dipole place at the center. We used free boundary conditions, which means the nodes at the boundary can move due to the contractile force generated from the dipole. First, we did some small runs with 2000 time-step as shown in Figure 3.2, and we tested the different plotting threshold for the spring forces. We decided to choose an intermediate value 10^{-6} as the default for the simulation to make sure the system is fully relaxed and the forces have propagated to the entire network without the values being too small to be negligible. With exactly 8185 steps, the contractile force appears to propagate throughout the network, and the total force magnitude measured by summing each node was roughly 2.55×10^{-4} . As our hypothesis predicted, the value is getting closer to zero with larger time-step, indicating the system is reaching its energy equilibrium as shown in Figure 3.3 c), d) and e), where each represents power, potential energy, and total force magnitude, respectively.

3.2 32x32 Network

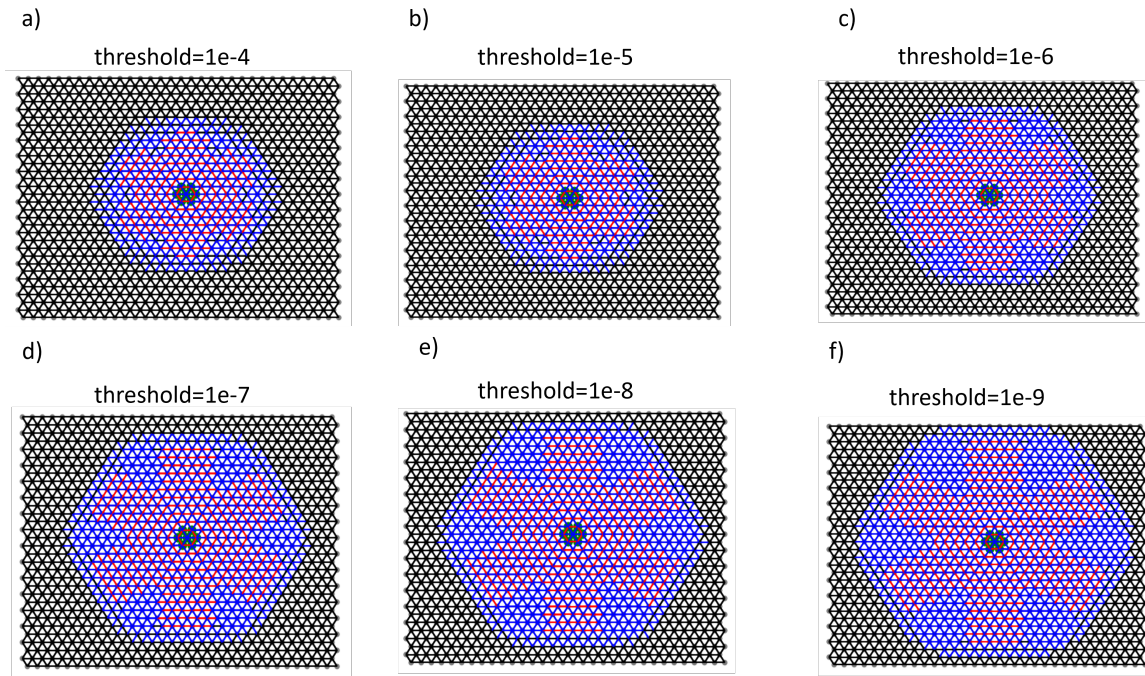


Figure 3.2 "Visualizing the strain on a 32x32 network after 2000 time-step at varying force thresholds, each reduced tenfold from a) threshold = 10^{-4} to f) threshold = 10^{-9} . As the threshold decreases, the propagation of forces is increasingly evident.

3.2 32x32 Network

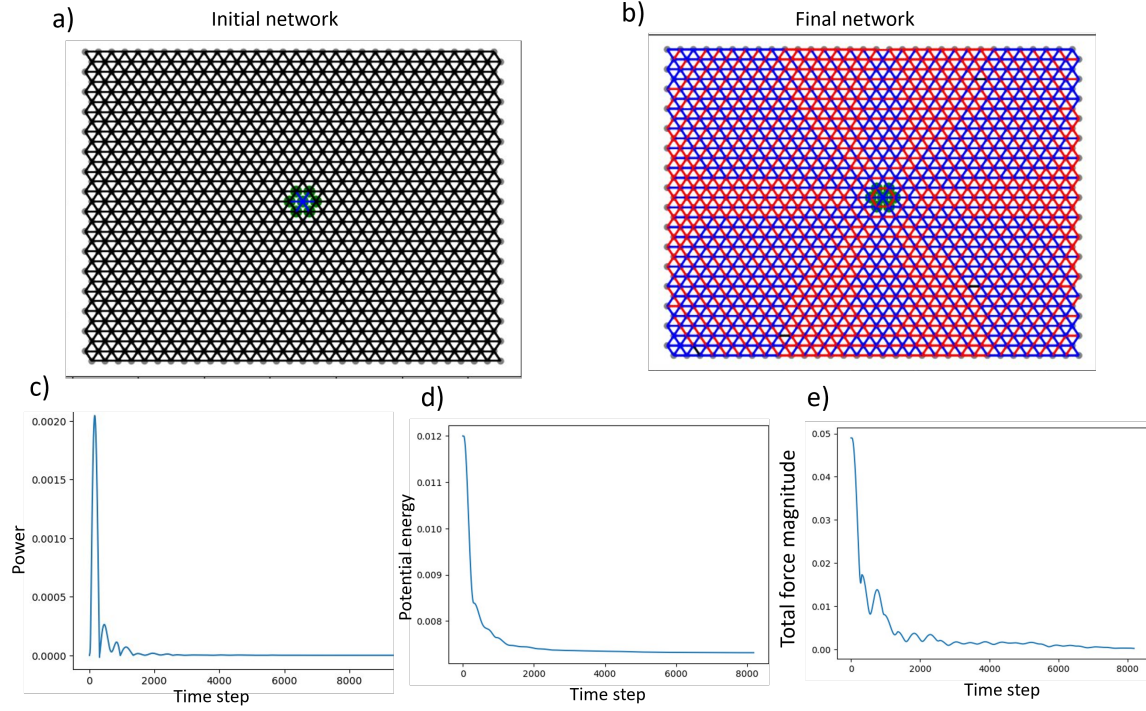


Figure 3.3 This figure shows: a) initializing a 32x32 network with a dipole in the middle; b) the bond patterns of the network after a simulation run of 8185 time-steps with plotting threshold= 10^{-6} ; c) the power of the network; d) the potential energy of the network; e) the total force magnitude of the network.

To better measure how the force has propagated through the entire network, we shifted to fixed circular boundary instead of free boundary. We created a circular region inscribed within the simulation box, and held all nodes on the boundary of the circle fixed during the simulation. The choice of a circular boundary is motivated by the isotropic nature of the force dipoles considered. We removed all the bonds outside the boundary so the node interactions only happen inside the boundary. We first tested out in a similar 32x32 network, and it produced similar plots of power, potential energy, and total force magnitude just as in the free boundary case. The boundary nodes are colored teal, and we can see the bonds between the boundary nodes remain black, indicating there was no displacement involved. (Figure 3.4)

3.3 64x64 Newwork and multiple dipoles

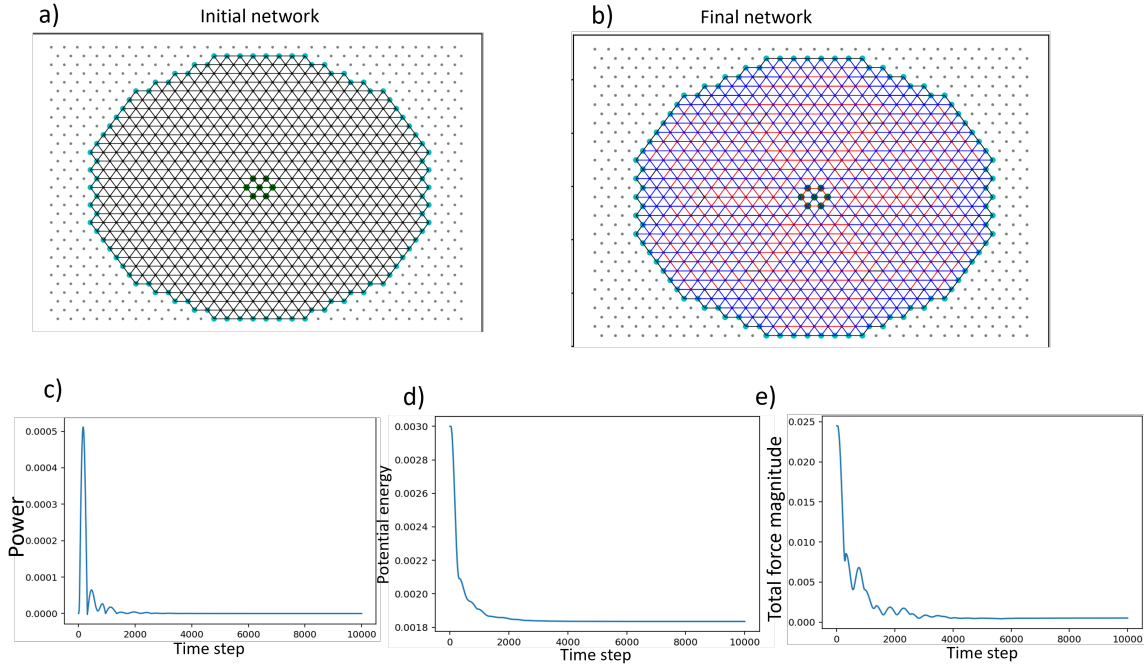


Figure 3.4

Fixed circular boundary condition for a 32x32 network. a) initializing a 32x32 network with a dipole in the middle; b) the bond patterns of the network after a simulation run of 10000 time-steps; c) the power of the network; d) the potential energy of the network; e) the total force magnitude of the network.

3.3 64x64 Newwork and multiple dipoles

To further increase the complexity of the network, we expanded it to the size of 64x64. This time, we calculate the dipole moment at the boundary by multiplying the radial forces measured at the boundary nodes and their radial distances from the center of the network, and we sum them up for the total dipole moment of the boundary. Once again, the plots show the similar patterns as the smaller networks, indicating the system is approaching equilibrium. (Figure 3.5)

3.3 64x64 Newwork and multiple dipoles

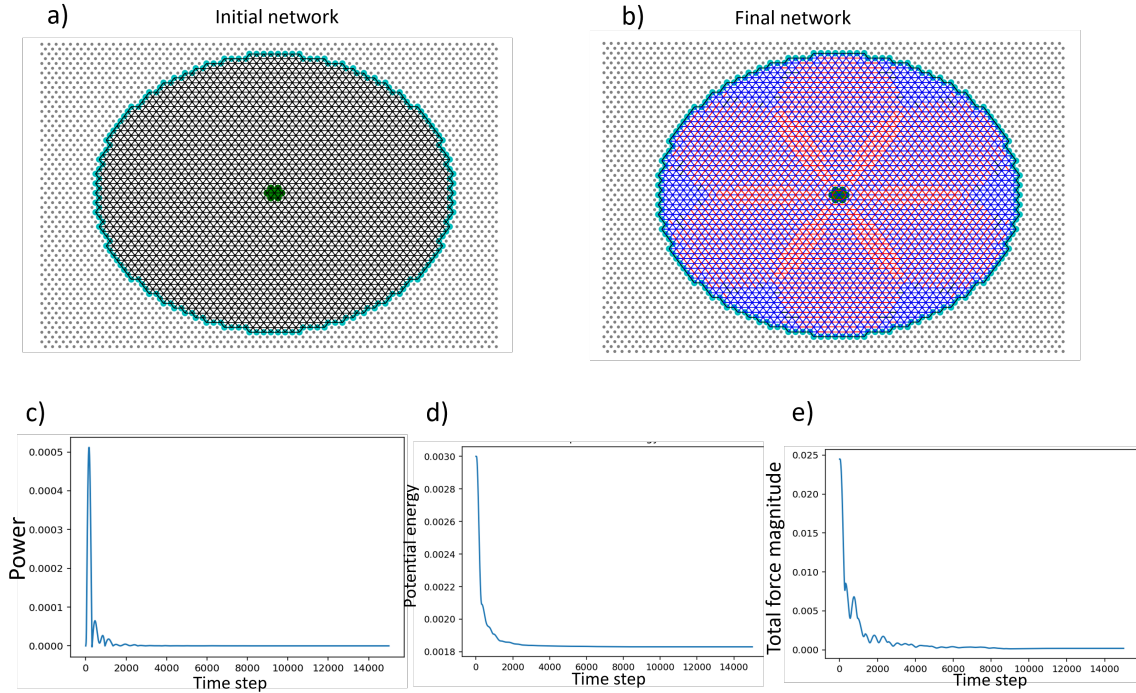


Figure 3.5

Fixed circular boundary condition for a 64x64 network. a) initializing a 64x64 network with a dipole in the middle; b) the bond patterns of the network after a simulation run of 15000 time-steps; c) the power of the network; d) the potential energy of the network; e) the total force magnitude of the network.

One dipole surely isn't enough to account for the numbers of myosin II in the network. So we added up to 5 dipoles where they're randomly placed inside the network, and they cannot be too close to one another since myosins have orderly stacking on the actins. We compared the number of dipoles and the total dipole moments measured at the boundary, and we found an almost perfectly linear relationship between the two variables, see Figure 3.6. This can be intuitively understood from an equivalent of the “Gauss’s law” in mechanics. Instead of electric fields and charges, we consider elastic stresses and forces. For force dipoles, this results in a “dipole conservation” principle for linear elastic media, where the net dipole moment measured at the boundary is equal

3.3 64x64 Newwork and multiple dipoles

to the sum of the applied local dipole moments of the active forces [5]. As a result, the total contractile (radially inward) boundary force depends linearly on number of force dipoles placed in the network, and is independent of where the dipoles are placed. However, further data points could be obtained where the dipoles are at different positions to further support this theory.

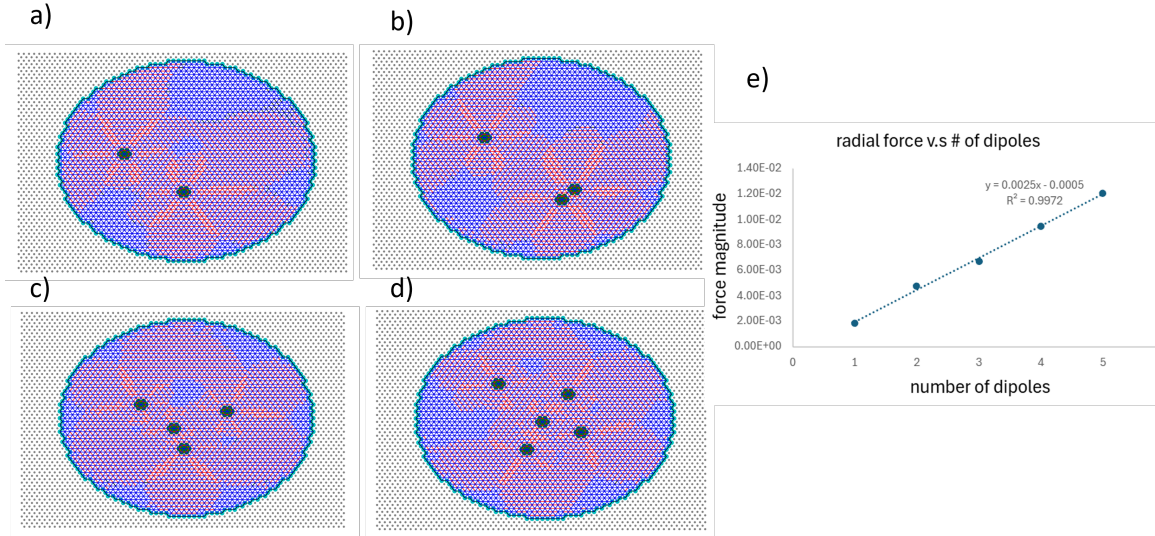


Figure 3.6 A collection of 2 or dipoles and their relationship with the radial forces measured at the boundary. a) 2 dipoles; b) 3 dipoles; c) 4 dipoles; d) 5 dipoles; and they all show the characteristic pattern of bonds stretching radially and compressing transversely. e) an approximate linear relationship between the number of dipoles and radial forces, with coefficient of determination $R^2 = 0.9972$. The line of best fit has the equation $y = 0.0025x - 0.0005$

Chapter 4

Conclusion

4.1 Summary

So far, we have shown that our realization of the FIRE algorithm gives expected configurations for an elastic spring network system, as the system gets close to mechanical equilibrium. This latter is tested through both the energy and total unbalanced force. We obtain characteristic patterns for force propagation from a single isotropic contractile force dipole, that have also been obtained by other computational methods such as conjugate gradient [4]. Through each network simulation, We see that the stretched bonds are always radially distributed and the compressed bonds are transversely distributed, no matter the positions of the dipoles.

However, when compare the dipole moment at the boundary to the dipole moment at the dipoles, the dipoles' values($dloc \approx 0.35207$) are more than 6 times greater than the boundary values($dfar \approx 0.04690$). We think this discrepancy occurs because network hasn't fully relaxed yet and requires more time steps. It is also possible the dipole moments calculated at dipoles weren't accurate to begin with. More results need to be produce to describe such disparity.

4.2 Future Work

4.2 Future Work

To better model the inherent disorder of the cytoskeleton network, we will randomly remove bonds from the network and introduce bending of the bonds to account for the angles among them. Currently, we are using $p = 1$, where all bonds are present, and we will vary this p value to see its effect on boundary forces. We already have some preliminary results of $p = 0.9$, but it requires further analysis, including increasing the number of dipoles and lower p values.(Figure 4.1). For $p < p_{cf} = 0.67$, we expect the network to become bending-dominated [1], in which case the dipole conservation principle will not hold [6]. This can lead to nonlinear dependency of contractile force at the boundary and the number of dipoles in the network.

In terms of simulation speed, as the network size gets bigger, the simulation time also increases drastically. First a 4x4 network takes less than 5 minutes, then a 32x32 network takes about half an hour, and a 64x64 network can take more than 2 hours to finish. Therefore, better coding script must be developed to improve the efficiency.

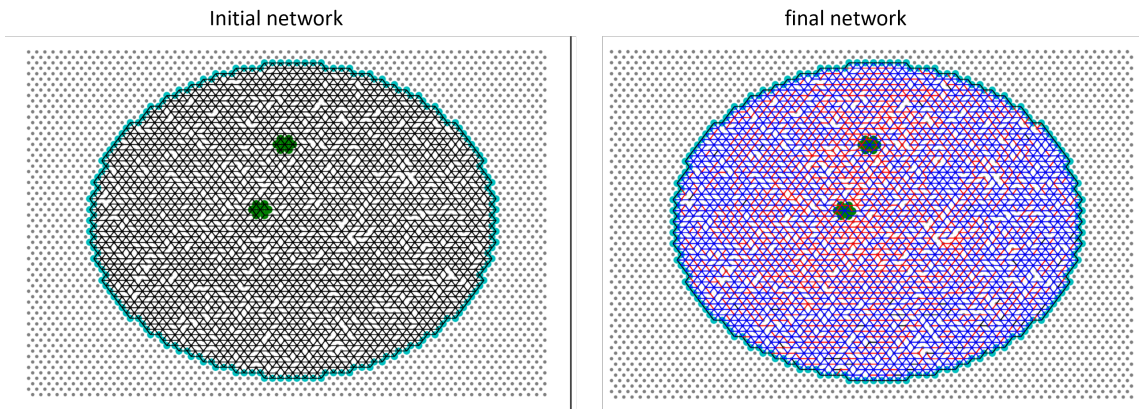


Figure 4.1 One premature result for $p= 0.9$ with two dipoles present.

Bibliography

- [1] C. P. Broedersz and F. C. MacKintosh, “Modeling semiflexible polymer networks,” *Rev. Mod. Phys.* **86**, 995–1036 (2014).
- [2] E. Bitzek, P. Koskinen, F. Gähler, M. Moseler, and P. Gumbsch, “Structural relaxation made simple,” *Physical review letters* **97**, 170201 (2006).
- [3] L. Blanchoin, R. Boujema-Paterski, C. Sykes, and J. Plastino, “Actin dynamics, architecture, and mechanics in cell motility,” *Physiological reviews* **94**, 235–263 (2014).
- [4] A. Kumar, D. A. Quint, and K. Dasbiswas, “Range and strength of mechanical interactions of force dipoles in elastic fiber networks,” *Soft Matter* **19**, 5805–5823 (2023).
- [5] P. Ronceray and M. Lenz, “Connecting local active forces to macroscopic stress in elastic media,” *Soft Matter* **11**, 1597–1605 (2015).
- [6] P. Ronceray, C. P. Broedersz, and M. Lenz, “Fiber networks amplify active stress,” *Proceedings of the National Academy of Sciences* **113**, 2827–2832 (2016).